Near Field Coupling Effects on Conducted EMI in Power Converter

Wei Chen, Limin Feng, Henlin Chen, Zhaoming Qian
College of Electrical Engineering, Zhejiang University
Hangzhou, 310027, China

yuxuan@zju.edu.cn

***Abstract* - In this paper, the effects of near field couplings including both magnetic coupling and electric coupling that exist in Boost PFC converter are analyzed and modeled. It is obvious that magnetic couplings have more significant effects on conducted DM noise than that of electric couplings. Based on the modeling of Boost inductor and capacitor, and estimating both inductive and capacitive couplings using Z parameters or Y parameters obtained by Ansoft HFSS software, the model of near field couplings is set up. This model is verified by comparison of simulated and measured voltage gains.**

I. INTRODUCTION

Near field couplings including magnetic and electric couplings between passive components in power converters have significant effects on EMI noise. Effects of parasitic parameters on the EMI filter performance have been investigated in paper [1]. It is obvious that the mutual coupling affects high frequency performance of EMI filters greatly. In paper [2], three methods of controlling parasitic couplings are analyzed and a novel method to reduce the parasitic parameter of capacitor is proposed. In paper [3] [4], the EMI filters are first characterized by Scattering parameters (S-parameters). Based on the network theory, S-parameters are utilized to extract the parasitic coupling in EMI filters. In paper [5], the boost inductor is modeled and the effects of inductive coupling on differential-mode (DM) conducted EMI are estimating by Maxwell 3D software.

In this paper, effects of near field couplings in a typical Boost PFC converter shown in Fig.1 on the differential mode (DM) conducted EMI are analyzed. Boost inductor L_{boost} is the main magnetic field source and node n1 is the main electric field source. Also, for magnetic couplings, there are two high frequency current loops, loop1 and loop2 shown in Fig.1. Since the reverse recovery current does not exist under critical DCM operating mode, the analysis in this paper mainly focus on the loop1. The models of L_{boost} and Cin are described in section II. The model of magnetic couplings is set up in section III. In this section, the inductive coupling is estimated by Z parameters of two-port-network using HFSS software, and measured and simulated voltage gains are compared. In section IV, the electric field couplings are modeled and parasitic capacitances are obtained by Y parameters. The whole near field couplings model is shown in section V, and it is concluded that electric field coupling has less effects on DM conducted noise than that of magnetic coupling.

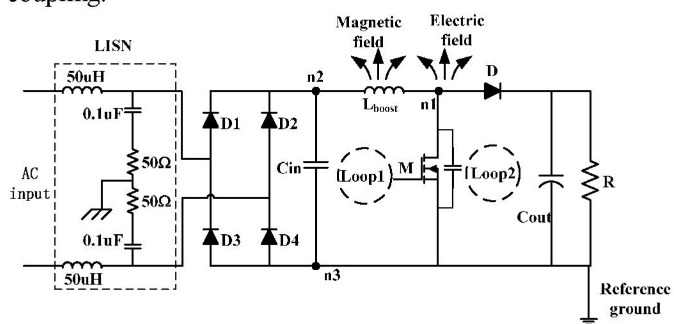

Fig.1 The power stage of typical Boost PFC

II. MODELING OF BOOST INDUCTOR L_{boost} AND CAPACITOR Cin

A. *Modeling of Boost inductor L_{boost}*

Due to the parasitic capacitances and the resistance of Boost inductor, the accurate inductor model is a complicated RLC networks in high frequency as shown in Fig.2, where L is the inductance per turn, R represents the core loss and C is the capacitance of adjacent turns. The other turn-to-turn capacitors are ignored.

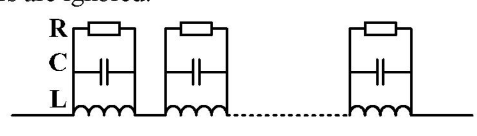

Fig.2 The model of inductor

This model is so complex that it is not easy to application. So a simple inductor model has to be developed. In Fig.3, the impedance of inductor is measured by network analyzer HP4195A which frequency range is from 100kHz to 30MHz.

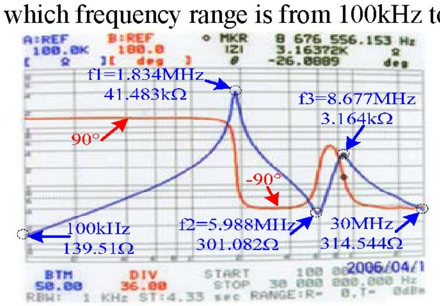

Fig.3 Measured impedance of inductor

Because there are two spikes at f1 and f3, the two RLC parallel unit model is enough in the frequency range which is given in Fig.4.

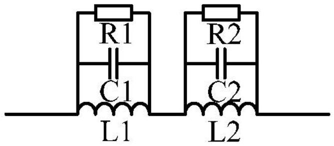

Fig.4 Simplified model of inductor

The first spike at f1 is caused by parallel resonant of L1 and C1, which values can be obtained HP4195A, L1=215.616uH and C1=34.4475pF. R1 is the value of impedance at f1, so R1=41.4827kΩ. Because the frequency f2 is far from f1, the second spick at f3 is mainly caused by resonant of C2 and L2, and R2=3.164kΩ.

The impedance of inductor according to Fig.4 is expressed in equation 1.

$$Z_L = \frac{1}{\dfrac{1}{R_1} + j\omega C_1 + \dfrac{1}{j\omega L_1}} + \frac{1}{\dfrac{1}{R_2} + j\omega C_2 + \dfrac{1}{j\omega L_2}} \qquad (1)$$

There are two unknown parameters in equation (1), L2 and C2. Two points in Fig.3 are selected to calculate L2 and C2, one point is at f2 and the other is at f3. They have to satisfy the following equations.

$$\left|Z_L\right|_{f=5.988MHz} = \left| \frac{1}{\dfrac{1}{R_1} + j2\pi fC_1 + \dfrac{1}{j2\pi fL_1}} + \frac{1}{\dfrac{1}{R_2} + j2\pi fC_2 + \dfrac{1}{j2\pi fL_2}} \right| = 301\Omega \qquad (2)$$

$$\left|Z_L\right|_{f=8.676MHz} = \left| \frac{1}{\dfrac{1}{R_1} + j2\pi fC_1 + \dfrac{1}{j2\pi fL_1}} + \frac{1}{\dfrac{1}{R_2} + j2\pi fC_2 + \dfrac{1}{j2\pi fL_2}} \right| = 3.164k\Omega$$

Both L2 and C2 can be solved according to equation (2), L2=12.6uH and C2=28.74pF.

Fig.5 shows the simulated impedance and phase curves. It is obvious that they match well with that in Fig.3.

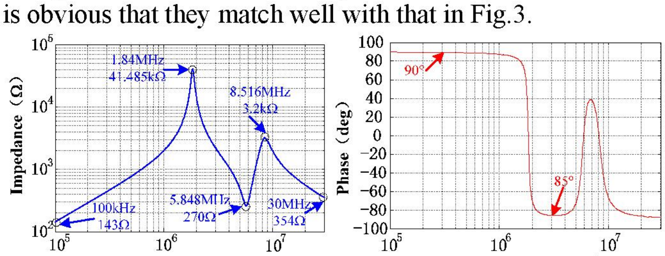

(a) Impedance vs. frequency (b) Phase vs. frequency

Fig.5 Simulated impedance of inductor

B. Modeling of capacitor Cin

Fig.6 is the high frequency equivalent circuit of capacitor. Both ESR and ESL are obtained using HP4195A, which values are: Cin=1.58uF, ESL=15.3nH, and ESR=18.1mΩ.

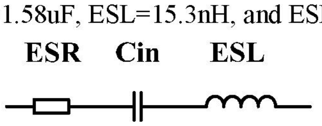

Fig.6 Model of capacitor

The measured and simulated results are shown in Fig.7 and Fig.8 respectively.

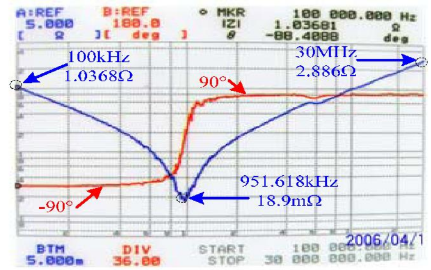

Fig.7 Measured impedance of capacitor

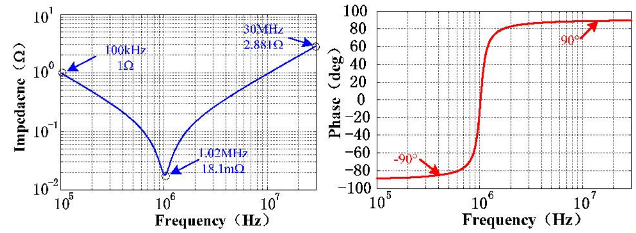

(a) Impedance vs. frequency (b) Phase vs. frequency

Fig.8 Simulated impedance of capacitor

III. Modeling Of The Magnetic Coupling

To reduce the influence of electric field coupling, the heatsink is not installed. According to Fig.1, the equivalent circuit of DM noise is modeled by a two-port-network as shown in Fig.9, in which the models of inductor and capacitor are considered and the magnetic coupling is not included. Lp1 and Lp2 are inductances of PCB loops, and Lp1=60nH and Lp2=30nH. Vn is the noise source and Vo is output voltage.

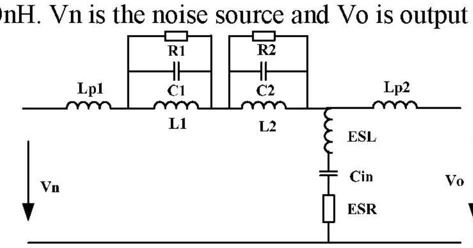

Fig.9 Equivalent circuit of DM noise (magnetic coupling is not considered)

The measured voltage gain and simulated voltage gain of the circuit are shown in Fig.10. It is obviously that they are different so much which is caused by magnetic couplings.

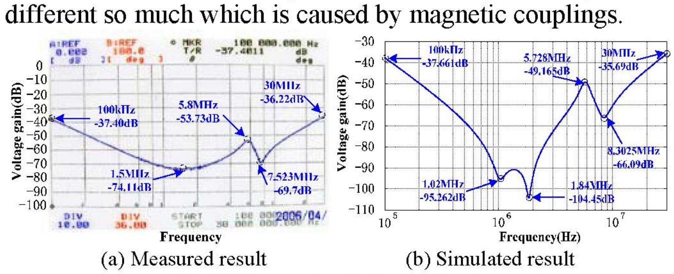

(a) Measured result (b) Simulated result

Fig.10 Measured and simulated voltage gains

A. Modeling of the magnetic coupling

The model considering the magnetic coupling is given in Fig.11. M_{11} and M_{12} are mutual inductances between inductor L1 and capacitor and between L2 and capacitor respectively. M_{21} and M_{22} are mutual inductances between L1 and Lp2 and between L2 and Lp2. M_3 is mutual inductance between Lp1 and Lp2. M_4 is mutual inductance between Lp1 and capacitor.

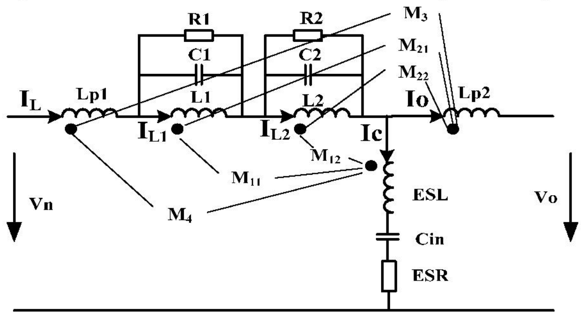

Fig.11 Equivalent circuit of DM noise considering the magnetic couplings

M_{11}, M_{12} and M_{21}, M_{22} should satisfy the following equations. M_1 is the total mutual inductance between inductor and capacitor and M_2 is the total mutual inductance between inductor and Lp2.

$$\begin{cases} M_1 = M_{11} + M_{12} \\ \dfrac{M_{11}}{M_{12}} = \dfrac{L_1}{L_2} \end{cases} \tag{3}$$

$$\begin{cases} M_2 = M_{21} + M_{22} \\ \dfrac{M_{21}}{M_{22}} = \dfrac{L_1}{L_2} \end{cases} \tag{4}$$

In addition, it can be observed that there exist positive coupling and negative coupling according to current direction of inductor, which are illustrated in Fig.12.

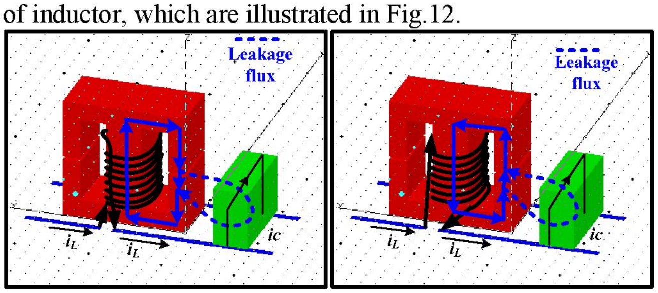

(a) Positive coupling (b) Negative coupling
Fig.12 Positive coupling and negative couplings between inductor and capacitor

B. Estimating the mutual inductances

How to obtain the mutual inductances is the key of magnetic coupling modeling. In this section, Z parameters is used to calculate the mutual inductances. Due to the same process, M_1 is calculated in detail here and the values of other mutual inductances are given directly.

To obtain M_1, the capacitor loop coupling the leakage flux of inductor has to be decided. Fig.13 shows the structure of the film capacitor. Notice that the cross section of capacitor is mainly metal poles of capacitor, so the loop of capacitor coupling the magnetic field is just shadow part in Fig.13 (b), which area is $A=w\times h$.

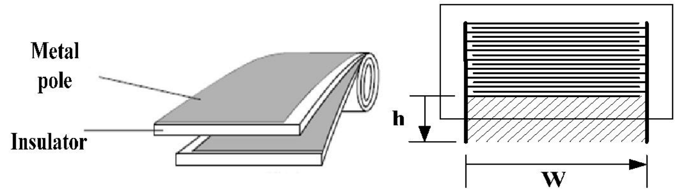

(a) Structure of film capacitor (b) Cross section of capacitor
Fig.13 Capacitor loop coupling magnetic field

Fig.14 shows the model in HFSS and its equivalent circuit. The metal plate is used to analog the pole of the capacitor.

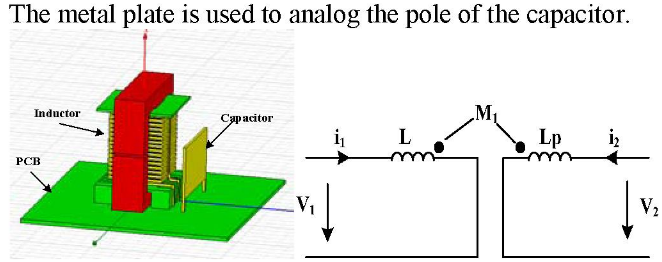

(a) Model in HFSS (b) Equivalent circuit
Fig.14 Model in HFSS and its equivalent circuit

According to the define of Z parameters of two-port-network, the Z parameters of this equivalent are expressed in equation (5),

$$\begin{cases} Z_{11} = \left.\dfrac{V_1}{i_1}\right|_{i_2=0} = j\omega L \\ Z_{12} = \left.\dfrac{V_1}{i_2}\right|_{i_1=0} = j\omega M_1 \\ Z_{12} = \left.\dfrac{V_2}{i_1}\right|_{i_2=0} = j\omega M_1 \\ Z_{22} = \left.\dfrac{V_2}{i_2}\right|_{i_1=0} = j\omega Lp \end{cases} \tag{5}$$

Notice that M_1 can be calculated by Z_{12} or Z_{21}. The values of M1 at four frequency points are given in table 1 and real parts of Z_{12} (Z_{21}) are neglected.

Table 1 Values of M_1

	$Z_{12}(Z_{21})$	M_1(nH)
1MHz	j0.1992	31.7
4MHz	j0.7812	31.08
7MHz	j1.565	35.58
10MHz	j2.1901	34.86

The mean value of four M1 at different frequency is used as the final result. It is,

$$M_1 = \frac{31.7+31.08+35.58+34.86}{4} = 33.305nH \tag{6}$$

And according to equation (3), M_{11}=31.467nH and M_{12}=1.839nH.

The other values of mutual inductances are given in table 2.

Table 2. Mutual inductanes in circuit

M_2(nH)		M_3(nH)		M_4(nH)	
M_{21}	M_{22}	Positive coupling	Negative coupling	Positive coupling	Negative coupling
4.878	0.285	-0.13	0.42	0.93	-1.96

According to the above analysis, the model of the circuit including the inductive couplings is set up in Fig.15.

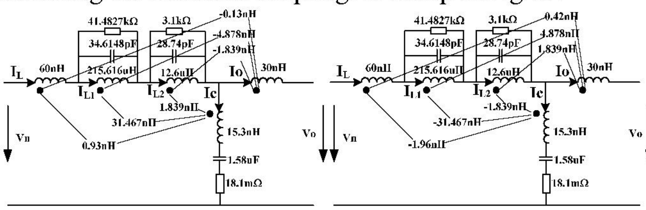

(a) Positive coupling (b) Negative coupling

Fig.15 Circuit model considering the magnetic couplings

The simulated results are compared with the measured results in Fig.16. It is obvious that they match very closely, which verifies the accuracy of this model.

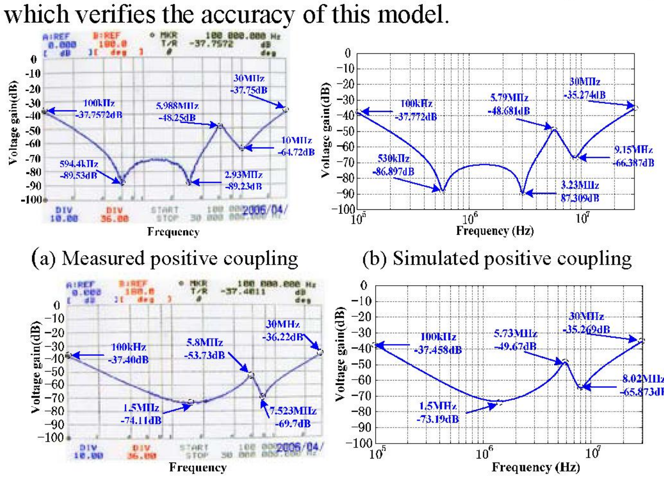

(a) Measured positive coupling (b) Simulated positive coupling

(c) Measured negative coupling (d) Simulated negative coupling

Fig.16 Measured and simulated voltage gain

IV. Modeling Of The Electrical Coupling

Besides the magnetic coupling, electric couplings also exist in power converter. For reducing the influences of magnetic couplings, the PFC inductor is removed from the Fig.1. The PCB traces are all at bottom layer and Mosfet is mounted on the heatsink. The equivalent circuit is shown in Fig.17. Cm is the parasitic capacitance between the Mosfet and heatsink, Cp1 is the parasitic capacitance between PCB traces connected to node n1 and heatsink, and Cp2 is the parasitic capacitance between PCB traces connected to n2 and heatsink. Cp3, Cp4 and Cp5 are the parasitic capacitances between two PCB traces as shown in Fig.17.

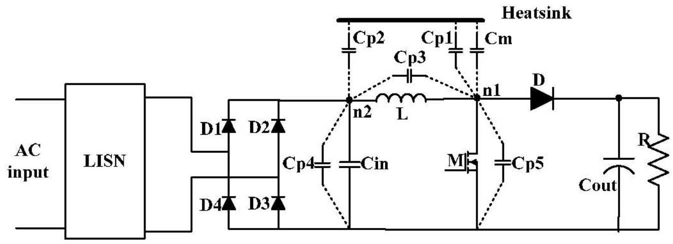

Fig.17 Circuit model considering the electrical couplings

Fig.18 is the equivalent circuit considering the electric couplings. Notice that the inductor are removed.

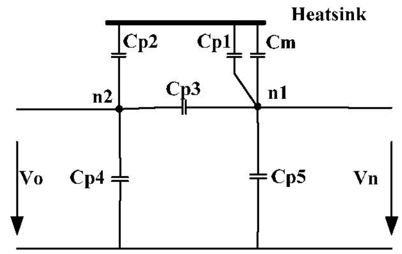

Fig.18 Equivalent circuit of capacitance coupling

The parasitic capacitance Cm can be measured directly, which value is Cm=30.29pF. The other parasitic capacitance can be calculated by Y parameters of π tpye network. In Fig.19, Cp3, Cp4 and Cp5 form a π network. Similarly, Cp3, Cp1 and Cp2 compose another π network. Here, we focus on calculating the Cp3, Cp4 and Cp5, and Cp1 and Cp2 will be given directly.

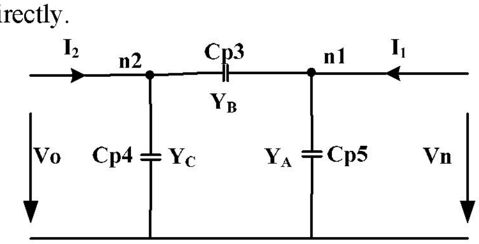

Fig.19 π network formed by Cp3, Cp4 and Cp5

According to Fig.19, the Y parameters of the π circuit can be drawn as equation (7).

$$\begin{cases} Y_{11} = \left.\dfrac{I_1}{V_n}\right|_{V_o=0} = Y_A + Y_B = j\omega(Cp3+Cp5) \\ Y_{12} = \left.\dfrac{I_1}{V_0}\right|_{V_n=0} = -Y_B = -j\omega Cp3 \\ Y_{21} = \left.\dfrac{I_2}{V_n}\right|_{V_o=0} = -Y_B = -j\omega Cp3 \\ Y_{22} = \left.\dfrac{I_2}{V_o}\right|_{V_n=0} = Y_B + Y_C = j\omega(Cp3+Cp4) \end{cases} \tag{7}$$

Cp3 can be calculated by Y_{12}, and then from Y_{11} and Y_{22}, Cp5 and Cp4 are obtained respectively.

Fig.20 shows the HFSS model for electric couplings. Because the PCB layouts of magnetic positive coupling and negative coupling are so similar that the paracitic capacitances are almost same, we only consider the positive coupling here.

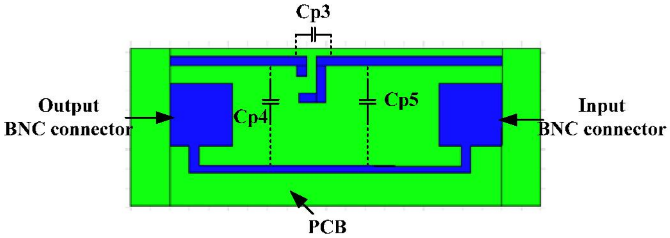

(a) PCB layout of positive coupling between inductor and capacitor

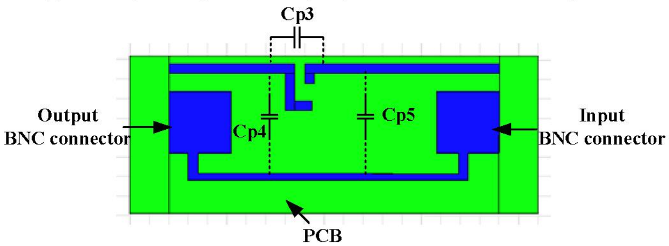

(b) PCB layout of negative coupling between inductor and capacitor
Fig.20 HFSS model of electrical coupling calculation

The simulated Y parameters are given in table 3. The real parts of Y parameters are also ignored.

Table 3 The calculated Y parameters

	$Y_{11}(\times10^{-3})$	$Y_{12}(\times10^{-4})$	$Y_{21}(\times10^{-4})$	$Y_{22}(\times10^{-3})$
1MHz	j0.02	-j0.02	-j0.02	j0.01
4MHz	j0.0801	-j0.0701	-j0.0701	j0.04
7MHz	j0.1402	-j0.1302	-j0.1302	j0.07
10MHz	j0.1904	-j0.1905	-j0.1905	j0.1001

According to table 3 and equation (7), the Cp3, Cp4 and Cp5 can be calculated which are shown in table 4 and mean values are used as the final results.

Table 4 The calculated parasitic capacitance

	Cp3(pF)	Cp4(pF)	Cp5(pF)
1MHz	0.3184	1.91	3.502
4MHz	0.2788	1.871	3.465
7MHz	0.2961	1.889	3.484
10MHz	0.3032	1.896	3.334
Mean value	0.2991	1.8915	3.4463

The Cp1 and Cp2 can be obtained using the same method, and the heatsink has to be modeled as shown in Fig.21, which values are: Cp1=2.8781pF, Cp2=1.4226pF.

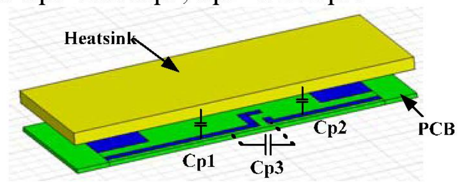

Fig.21 HFSS model for Cp1and Cp2 calculation

Fig.22 shows the equivalent electrical coupling circuit. Ceq is equal to equation (8).

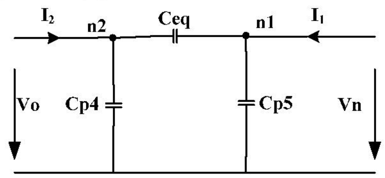

Fig.22 Equivalent circuit of electrical coupling

$$Ceq = Cp3 + \frac{(Cm + Cp1)Cp2}{Cm + Cp1 + Cp2} = 1.3641pF \qquad (8)$$

The measured and simulated voltage gain are given in Fig.23. It is obviously that they match well in frequency range from 100kHz to 30MHz.

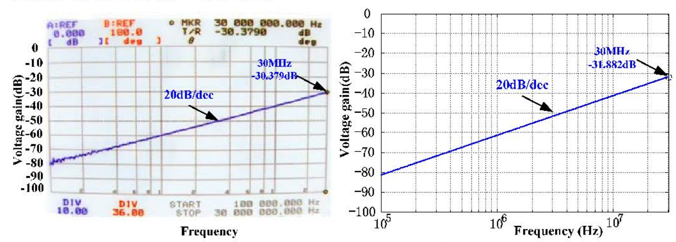

(a) Measured voltage gain (b) Simulated voltage gain
Fig.23 Comprison of measured and simulated voltage gain

V. Modeling Of The Near Field Coupling

Based on the modeling of magnetic coupling and electrical coupling, the whole model of near field coupling can be obtained which is shown in Fig.24.

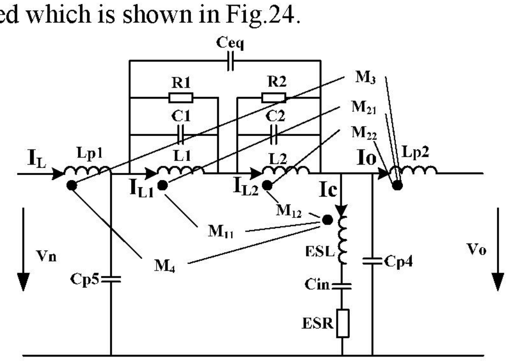

Fig.24 The near field coupling model

The measured and simulated voltage gain are given in Fig.25. It can be observed that the results match well for positive coupling and negative coupling.

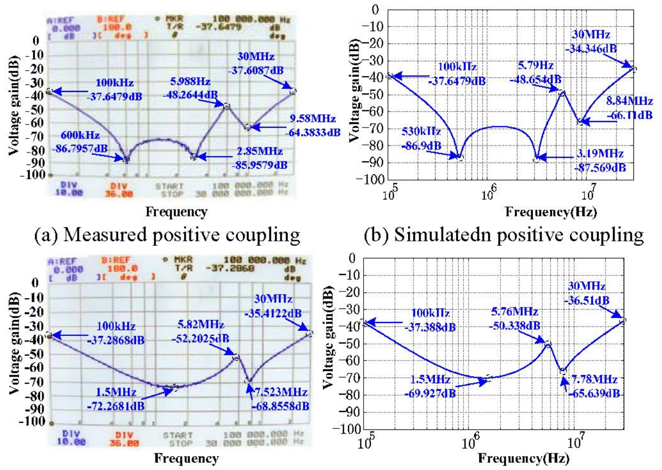

(a) Measured positive coupling (b) Simulatedn positive coupling

(c) Measured negative coupling (d) Simulated negative coupling

Fig.25 Measured and simulated voltage gain of near field coupling

It also can be drawn that magnetic coupling has more great influence on DM noise than that of electrical coupling. Fig.26 is the comprison of simulated voltage gains with and without electrical coupling. It is found that the voltage gain only increase 1dB above 8MHz when electrical coupling is considered.

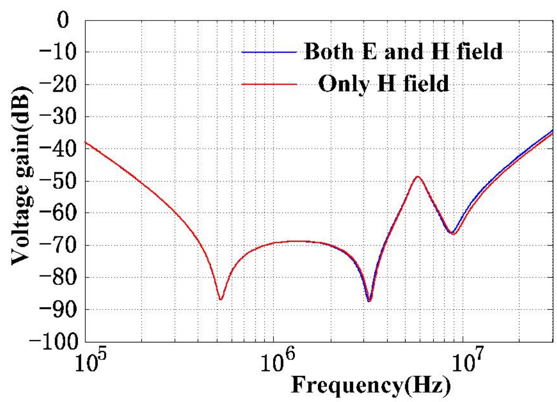

Fig.26 Comprison of voltage gains with and without electrical coupling

VI. Conclusion

In this paper, the effects of near field couplings including both magnetic coupling and electrical coupling that exist in Boost PFC converter are analyzed and modeled. It can be concluded that magnetic couplings have more significant effects on conducted DM noise than that of electric couplings. Based on the modeling of Boost inductor and capacitor, the mutual inductances are estimated by using Z parameters which are obtained by Ansoft HFSS software. Also, the parasitic capacitances are extracted by calculated Y parameters. The measured and simulated results match well each other in frequency range from 100kHz to 30MHz. Finally, the model of near field couplings is set up according to magnetic and electrical coupling respectively. This model is verified by comparison of simulated and measured voltage gains.

Acknowledgement

This work is supported by Natural Science Foundation of China (50077020).

Reference

[1] Shuo Wang, etc. “Effects of parasitic parameters on the performance of EMI filters,” *IEEE Trans. Power Electron.*, vol.19, no.3, pp.869-877, May 2004.

[2] Shuo Wang, etc. “Controlling the parasitic parameters to improve EMI filter performance,” in *Proc. IEEE Applied Power Electronics Conf.*, vol.1, Anaheim, CA, Feb.22-26, 2004, pp.503-509.

[3] Shuo Wang, etc. “Using scattering parameters to characterize EMI filters,” in *Proc. IEEE Power Electronics Specialists Conf.*, Aachen, Germany, Jun.20-25, 2004, pp.297-303.

[4] Shuo Wang, etc. “Characterization and parasitic extraction of EMI filters using scattering parameters,” *IEEE Trans. Power Electron.*, vol.20, no.2, pp.502-510, March 2005.

[5] Wei Chen, etc. “Analysis the inductance coupling effects on the differential mode EMI in power converter”, in *Proc. IEEE Applied Power Electronics Conf.*, USA, March 19-24, 2006